**Common and distinct drivers of convective mass flux and Walker circulation changes**

Sarah M. Kang[1], Masahiro Watanabe[2], and Veronika Gayler[1]

[1]Max Planck Institute for Meteorology, Hamburg, Germany

[2]Atmosphere and Ocean Research Institute, University of Tokyo, Kashiwa, Japan

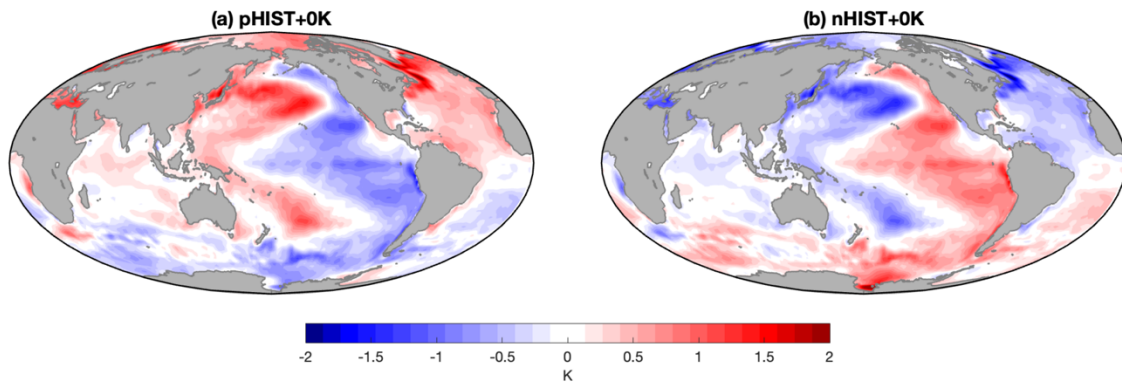**Contents of this file**

Figures S1 to S5

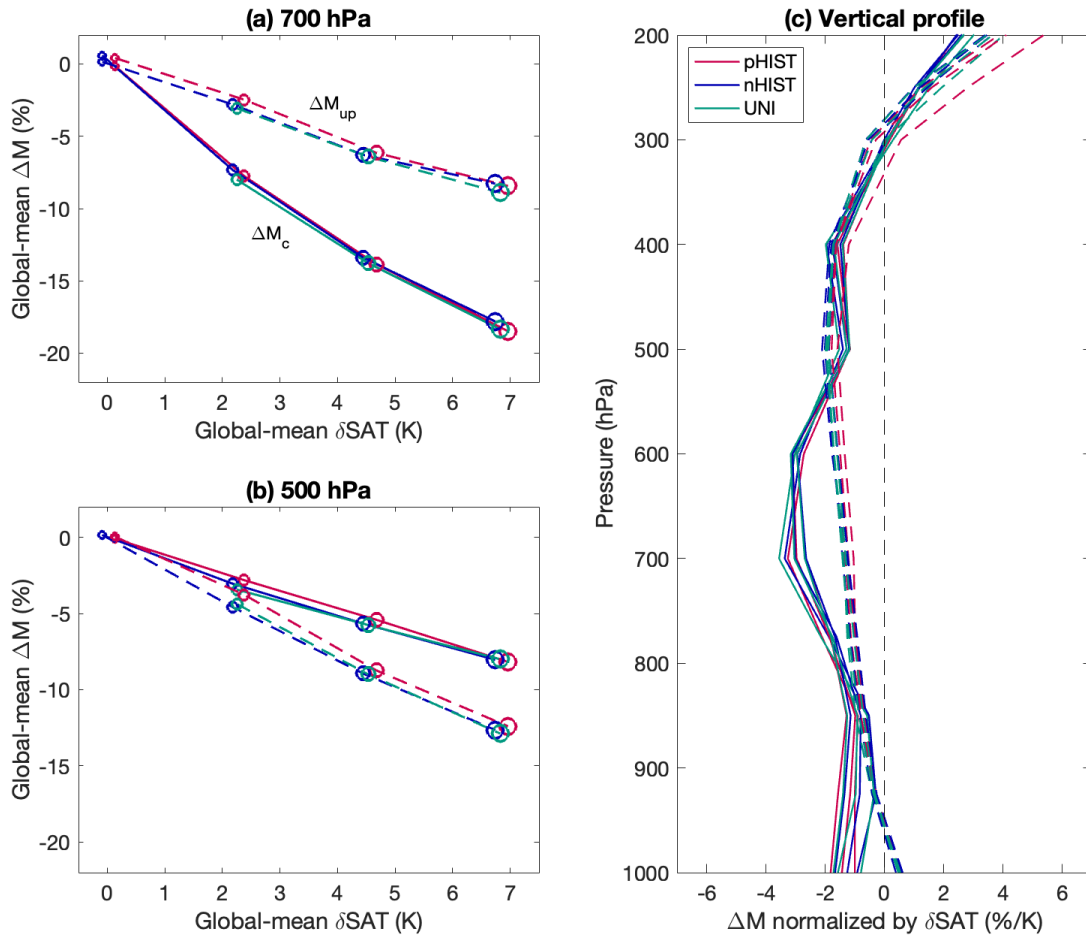**Figure S1.** Prescribed SST anomaly (in K) in (a) pHIST+0K and (b) nHIST+0K.

**Figure S2.** Fractional change in global-mean sub-grid convective mass flux $M_c$ (solid) and resolved mass flux $M_{up}$ (dashed) at (a) 700 hPa and (b) 500 hPa. (c) Vertical profile of fractional change in global-mean convective mass flux normalized by global-mean surface air temperature change. The experiments with pHIST SST pattern changes in red, nHIST SST pattern changes in blue, and uniform SST warming in green. The size of circle symbols corresponds to the prescribed global-mean SST warming amplitude (i.e., 0K, +2K, +4K, and +6K).
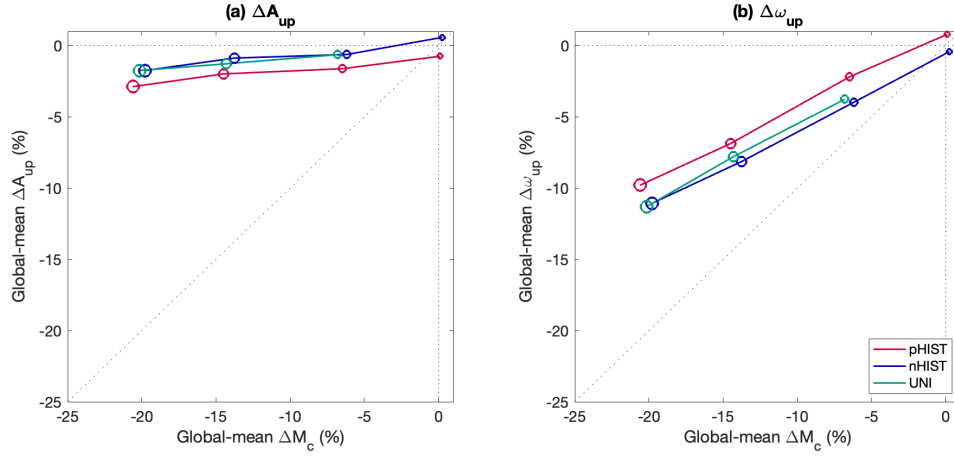
**Figure S3.** Fractional change in (a) $A_{\mathrm{up}}$, the fraction of the globe covered by ascent and (b) $\omega_{\mathrm{up}}$, the global-mean ascending pressure velocity with the reversed sign. Figure format same as in Figure S1.
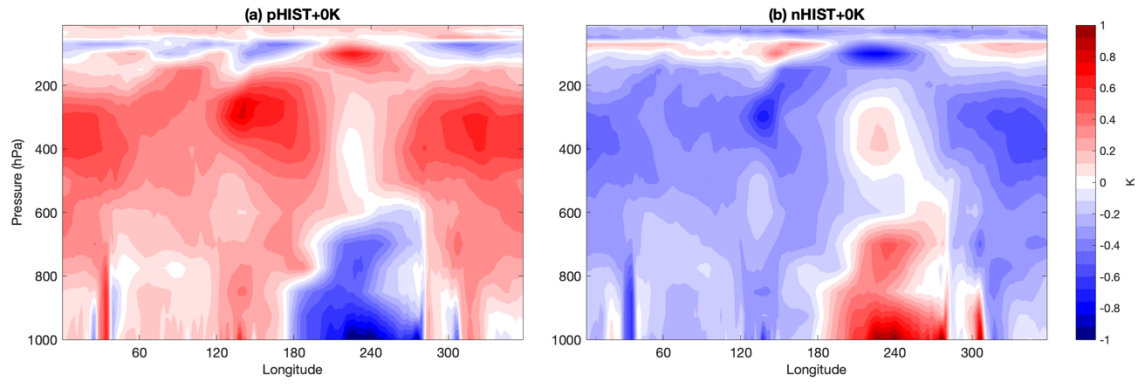
**Figure S4.** Temperature change (in K) in the equatorial band averaged between 2°S and 2°N in (a) pHIST+0K and (b) nHIST+0K.
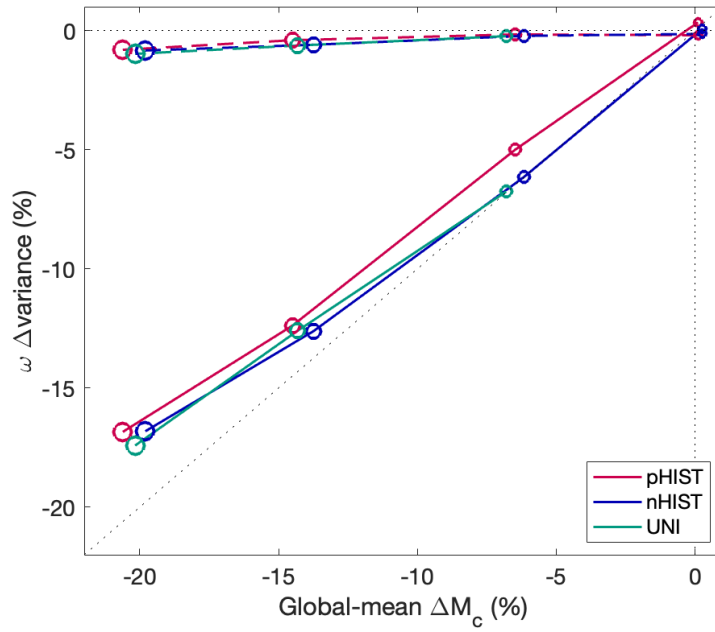
**Figure S5.** Fractional change in global-mean sub-grid convective mass flux at 600 hPa, $\Delta M_c$, compared with fractional change in global-mean spatial variance of daily $\omega$ at 600 hPa, decomposed into the zonal-mean (dashed) and zonally asymmetric (solid) components.